

Supporting Information For:

Molecular cobalt electrocatalyst for proton reduction at low overpotential

Hyun S. Ahn, Timothy C. Davenport, and T. Don Tilley*

Contribution from the Department of Chemistry University of California, Berkeley, Berkeley, California 94720, and the Chemical Sciences Division, Lawrence Berkeley National Laboratory, 1 Cyclotron Road, Berkeley, California, 94720.

Email: tdtilley@berkeley.edu

Table of Contents	Page
Experimental	2-4
¹ H NMR and ¹⁹ F NMR spectra of 1 and 2 (Figure S1)	5
CV of 2 with the central Co ^{III/II} redox (Figure S2)	6
Faradaic Efficiency Calculations	7
Faradaic Efficiency Measurement at $\eta = 225$ mV (Figure S3)	8
Faradaic Efficiency Measurement at $\eta = 275$ mV (Figure S4)	9
i vs $v^{1/2}$ plot for measurement of the diffusion coefficient of 2 (Figure S5)	10
Estimation of the diffusion coefficient and TOF of 2	11
CV of 1 with added acid (Figure S6)	12
CVs of 2 in catalysis at various rotation rates (Figure S7)	13
Koutecky-Levich plot for the proton reduction catalysis of 2 (Figure S8)	14
DPV of 2 (Figure S9)	15
CV of [Co(tpm) ₂]-2BF ₄ with added acid (Figures S10)	16
UV-vis spectra of 1 and 2 (Figure S11)	17
Catalytic current expressed as a function of tosic acid concentration (Figure S12)	18
Crystallographic data for the structure of 1 (Tables S1-S5)	19-30
References	31

Experimental

General. All manipulations were conducted under an inert nitrogen atmosphere using standard Schlenk techniques or a Vacuum Atmospheres drybox, unless otherwise stated. Chemicals were purchased from Aldrich and used as received. Dry, oxygen free solvents were used throughout. The compound $\text{Co}[\text{N}(\text{SiMe}_3)_2]_2$ ¹ was synthesized as reported in the literature. Carbon, hydrogen, and nitrogen elemental analyses were performed at the College of Chemistry microanalysis laboratory at the University of California, Berkeley. FTIR spectra were obtained on a Thermo Nicolet 6700 FTIR spectrometer. The UV-Vis spectra were acquired using a Varian Cary 300 series spectrometer. Transmission electron microscopy (TEM) was carried out on a Philips Tecnai 12 transmission electron microscope operating at 200 kV. Inductively coupled plasma optical emission spectroscopy (ICP-OES) for cobalt ion detection in post catalytic solutions was performed on a Perkin-Elmer ICP-OES Optima 7000 DV. Standard solutions were purchased from Perkin-Elmer and used as received. Electrochemical data were recorded on a Bioanalytical Systems model EC epsilon computer-controlled potentiostat. Unless otherwise stated, all measurements were conducted in a 25 mL glass cell with a three-electrode configuration. Electrochemistry experiments were performed in HPLC grade acetonitrile solutions with 0.1 M $\text{N}(\text{nBu})_4\text{PF}_6$. The reference electrode used was 0.1 M $\text{Ag}/\text{Ag}(\text{NO}_3)_3$ in acetonitrile and the reference was calibrated relative to ferrocene/ferrocenium in order to correct for any potential drifts for every data collection. Solution resistance in CV and LSV experiments was corrected for by the iR compensation algorithm, using software in the EC epsilon potentiostat. Polished platinum wire was used as an auxiliary electrode, and glassy carbon working electrode with a 3 mm diameter was utilized. Rotating disk electrode experiments were performed using the Bioanalytical Systems model RDE-2 unit. Faradaic efficiencies were

determined by observing H₂ production by Agilent GC using a gas separation column. An aliquot of headspace gas (100 μL) was extracted with a gas-tight syringe after the electrolysis experiment and injected into a GC sample port manually. Solution ¹H NMR and ¹⁹F NMR spectra were recorded at 400 MHz using a Bruker AVQ-400 spectrometer. Chemical shifts for ¹H NMR spectra were referenced internally to the residual solvent proton signal relative to tetramethylsilane. Chemical shifts for ¹⁹F NMR spectra were referenced internally to the residual solvent proton signal relative to trichloro-fluoro-methane. X-ray diffraction data were collected using a Bruker AXS three-circle diffractometer coupled to a CCD detector with graphite-monochromated Mo K α radiation ($\lambda = 0.71073 \text{ \AA}$). The structures were solved by direct methods using SHELXS and refined against F^2 on all data by full-matrix least squares with SHELXL-97. All non-hydrogen atoms were refined anisotropically; hydrogen atoms were included into the model at their geometrically calculated positions and refined using a riding model. Experimental details of the crystal structure for compound (**1**) are given in Table S1-S5. Additional details can be found in the CIF file available as electronic supplementary material.

Synthesis of [Co₃(C₅H₉O₂)₆][BF₄]₂ (1**).** In a typical synthesis, Co[N(SiMe₃)₂]₂ (380 mg, 1 mmol) was dissolved in THF (ca. 30 mL). A THF (20 mL) solution of AgBF₄ (136 mg, 0.7 mmol) was then added. After stirring the mixture at room temperature for 10 min, 307 mg (3 mmol) of 3-hydroxy-3-methyl-2-butanone (HOCMe₂COMe) was added dropwise. The reaction mixture was then heated to 55 °C for 8 h. A slow color change to red was observed. The solution was filtered and the solvent was removed under vacuum and the resulting solid was washed with hexanes three times (30 mL each wash) and ether three times (30 mL each wash). The product was obtained in 85% yield by recrystallization in THF by concentration and cooling to -78 °C under N₂. The identical compound was obtained in similar yields when ferrocenium

tetrafluoroborate was employed as the oxidant. Anal. Calcd: C, 37.65; H, 5.69; Co, 18.47.

Found: C, 37.21; H, 5.70; Co, 18.00. ^1H NMR (400.13 MHz, CD_3CN): δ = 70.70 (s), 14.27 (s, THF), 12.91 (s, THF), -97.14 (s). ^{19}F NMR (376.49 MHz, CD_3CN): δ = -147.9 (s). IR (KBr, cm^{-1}) 3295 (m), 2979 (m), 2932 (m), 1658 (s), 1463 (m), 1437 (m), 1380 (s), 1356 (m), 1286 (w), 1170 (s), 1042 (s), 963 (bs), 885 (m), 842 (m), 764 (s).

Synthesis of $[\text{Co}_3(\text{C}_6\text{H}_{11}\text{O}_2)_6][\text{BF}_4]_2$ (2). Synthetic procedures were identical to those used for **1**, with 4-hydroxy-4-methyl-2-pentanone ($\text{HO}(\text{CMe}_2\text{CH}_2\text{C}(\text{O})\text{Me})$) as the source of the ligand. The solvent was removed under vacuum and the resulting solid was washed with hexanes three times (30 mL each wash) and ether three times (30 mL each wash). Analytically pure product was obtained in 76% yield. Anal. Calcd: C, 41.52; H, 6.39; Co, 16.98. Found: C, 41.90; H, 6.72; Co, 17.01. ^1H NMR (400.13 MHz, CD_3CN): δ = 66.73 (s), 36.01 (s, THF), 13.12 (s, THF), -7.04 (s), -95.41 (s). ^{19}F NMR (376.49 MHz, CD_3CN): δ = -148.2 (s). IR (KBr, cm^{-1}) 3285 (w), 2969 (w), 1658 (s), 1594 (m), 1522 (w), 1466 (m), 1429 (m), 1374 (m), 1285 (w), 1247 (w), 1223 (w), 1054 (s), 1026 (s), 875 (s), 837 (s), 752 (s).

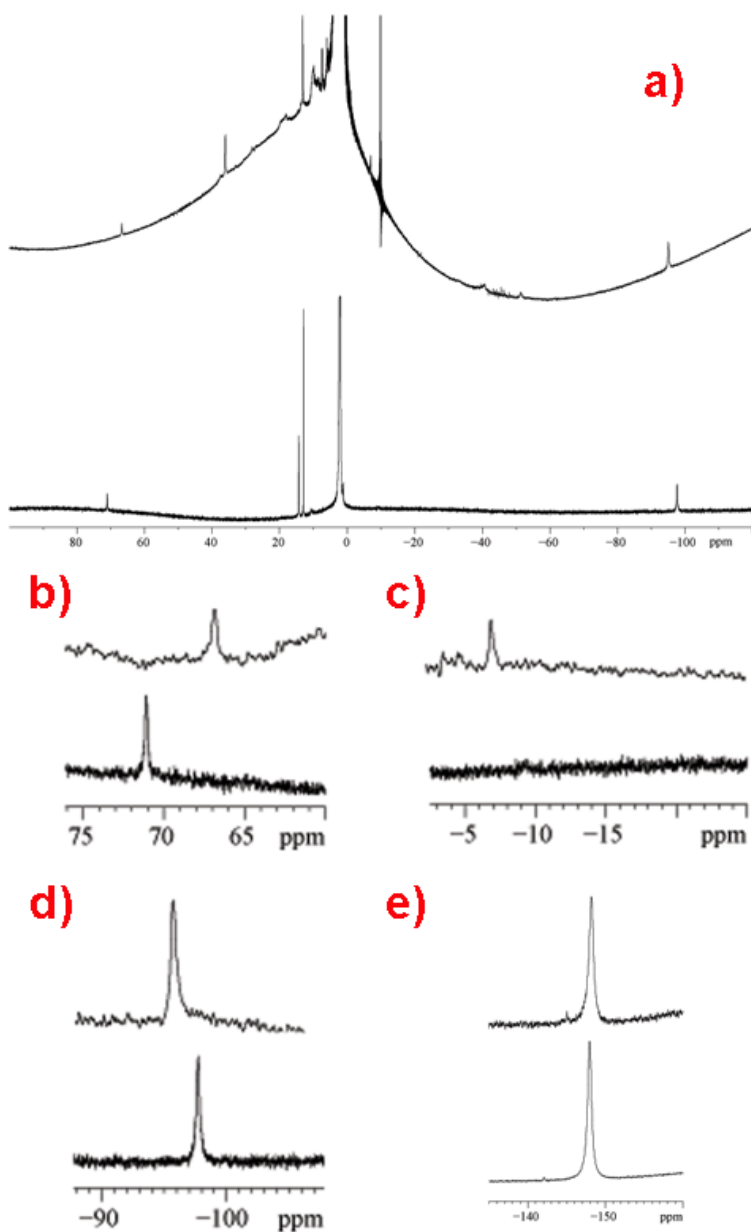


Figure S1. a) Paramagnetic ^1H NMR spectra of **1** (bottom) and **2** (top). Important sections of the spectra are highlighted in b), c), and d). Two of the methyl group protons on the ligand are displayed in b) and d), respectively, and the corresponding signals for **1** and **2** exhibit similar chemical shifts. Methylene protons unique to **2** appear at ca. -7.04 ppm, as shown in c). ^{19}F NMR spectra of **1** (bottom) and **2** (top) are displayed in e). Signals at ca. -148 ppm appear at a nearly identical chemical shift and are clearly distinct from that of $\text{Co}(\text{BF}_4)_2$, which appears at -134 ppm.

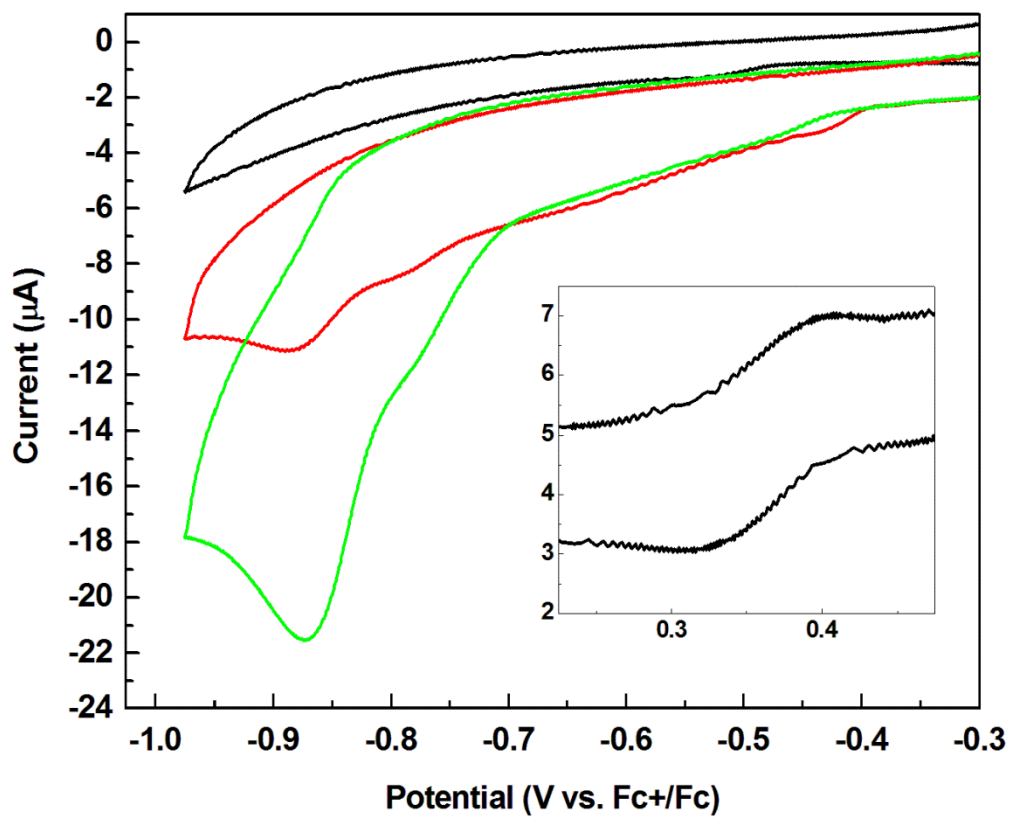


Figure S2. CV of 2 in the presence of HOTs (0 mM, 5 mM, and 9 mM). Shown in the inset is the reversible Co^{III/II} couple.

Faradaic Efficiency Calculation

Faradaic efficiencies for the proton reduction catalyses by compound **2** were calculated simply by dividing the GC measured quantity of H₂ by the theoretical amount of H₂ based on the charge passed during electrolyses. The theoretical amount of H₂ was calculated by the following equation:

$$\text{Total charge passed during electrolysis [C]} \times \frac{6.241 \times 10^{18} \text{ e}^-}{1 \text{ C}} \times \frac{1 \text{ H}_2}{2 \text{ e}^-} \times \frac{1 \text{ mol H}_2}{6.022 \times 10^{23} \text{ H}_2} =$$

Theoretical H₂ Yield [mol H₂]

Generally, GC measurements were made after ca. 10 C had passed in an electrolysis experiment, corresponding to ca. 2.2 turnovers for all catalyst molecules in solution. The actual turnover number is expected to be much greater than 2 because only the catalysts near the electrode surface (much lower number compared to those in the bulk) participate in catalysis.

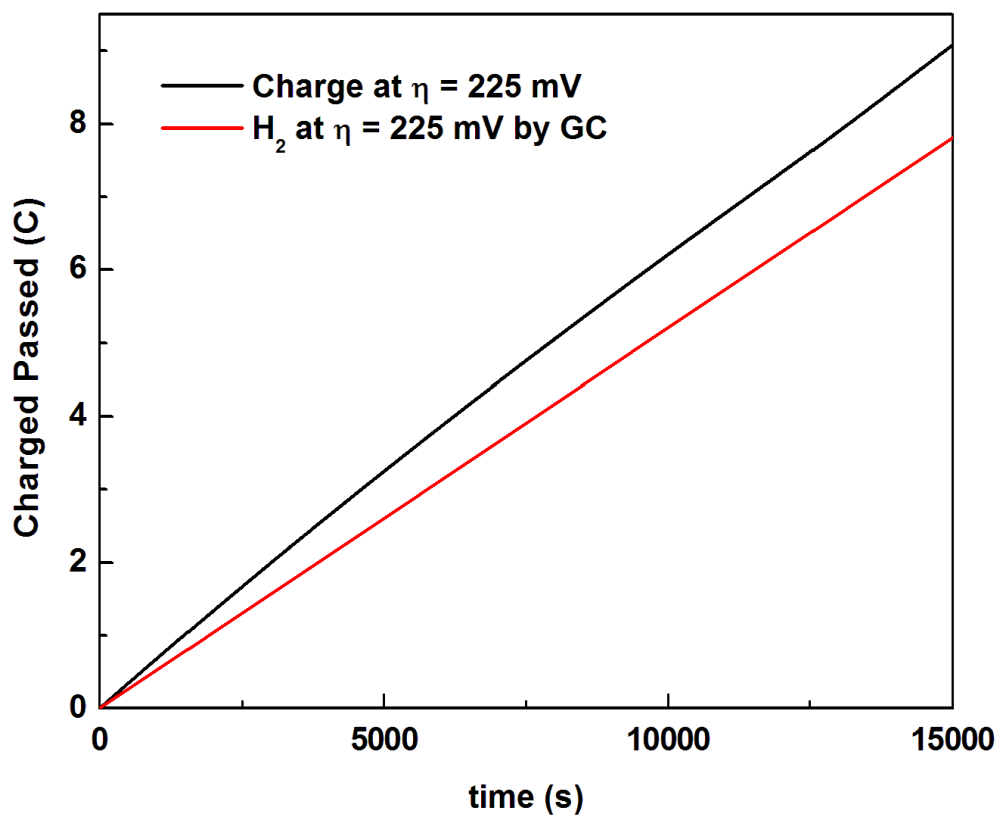


Figure S3. Charge passed (black trace) at an electrolysis experiment performed at $\eta = 225$ mV. The amount of H_2 observed by GC measurement was converted to the amount of charge required to produce the observed amount of H_2 , and plotted in red. The Faradaic efficiency calculated for this electrolysis experiment is 83 %.

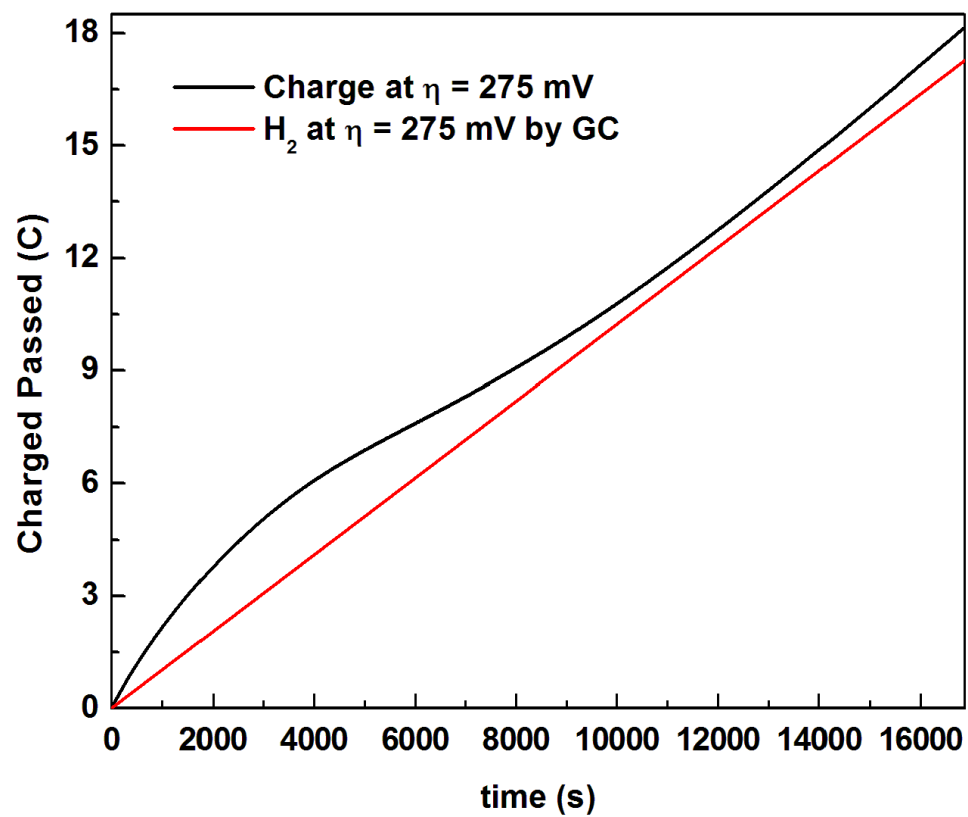


Figure S4. Charge passed (black trace) at an electrolysis experiment performed at $\eta = 275$ mV. The amount of H₂ observed by GC measurement was converted to the amount of charge required to produce the observed amount of H₂, and plotted in red. The Faradaic efficiency calculated for this electrolysis experiment is 86 %.

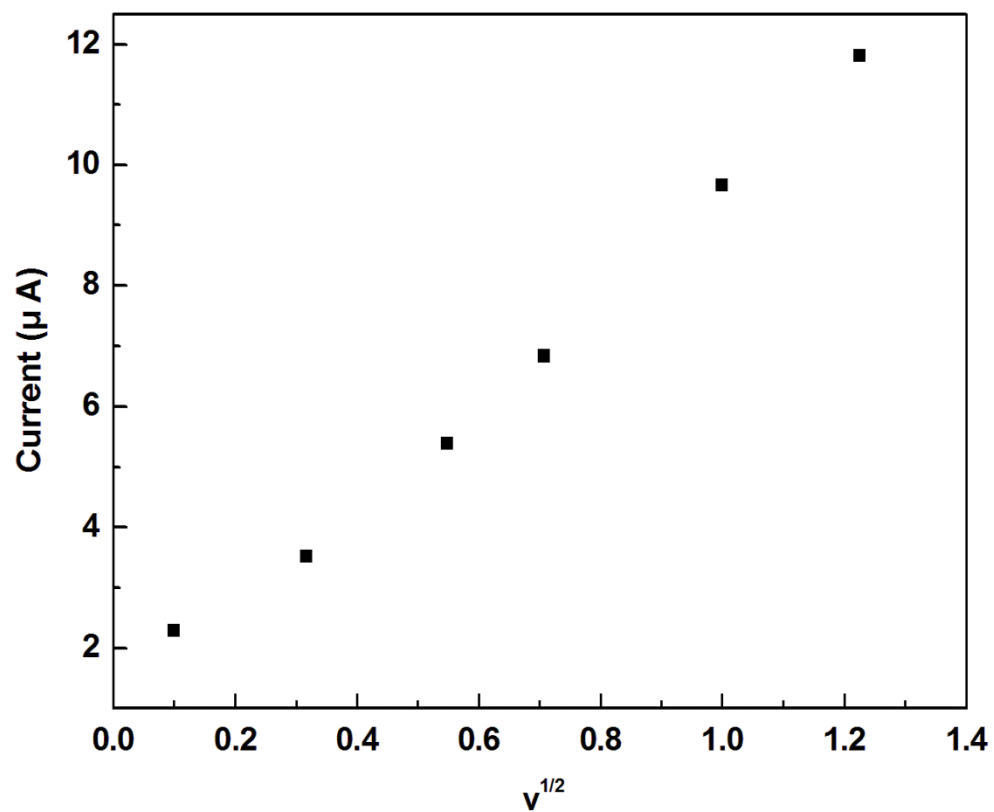


Figure S5. Anodic peak current for the $\text{Co}^{\text{III/II}}$ in compound **2** is plotted as a function of the squared root of the scan rate. The data was collected in order to estimate the diffusion coefficient for the complex (see page 11 of the SI).

Diffusion Coefficient and TOF Estimation

The diffusion coefficient for compound **2** in the reaction solution was estimated electrochemically. The Co^{III/II} couple was measured at varying scan rates (data in Figure S5), and the diffusion coefficient for compound **2** was deduced from the data according to the following relationship:

$$i_p = 0.4463 \left(\frac{F^3}{RT} \right)^{1/2} n^{3/2} A D^{1/2} C v^{1/2}$$

In the above equation, i_p is the peak current of the electrochemical event of interest (in this case, Co^{II} → Co^{III}), F is Faraday's constant, n is the number of electrons involved in the electrochemical event of interest, A is the area of the electrode, C is the concentration of the analyte, D is the diffusion coefficient of the analyte, and v is the scan rate. For detailed derivation of the equation, refer to chapter 6 of reference 2.

The diffusion coefficient of **2** obtained from the data presented in Figure S5 by the mathematical relationship described above is ca. $6.0 \times 10^{-6} \text{ cm}^2 \text{ s}^{-1}$.

The TOF of proton reduction catalysis by **2** was calculated by the following expression derived by Kubiak and coworkers for a homogeneous catalytic system assuming an EC' mechanism.³

$$\text{TOF} = \frac{1}{D_c} \left(\frac{j_{lim}}{nF[C]} \right)^2$$

D_c is the diffusion coefficient of the catalyst (obtained in calculations above). j_{lim} is the limiting current density at diffusion limited potentials, and in our case a peak current at $\eta = 300 \text{ mV}$ was selected. An example calculation is as follows:

$$\text{TOF} = \frac{1}{(6.0 \times 10^{-6})} \left(\frac{0.0017 \text{ A/cm}^2}{2 e^- \times 96485 \text{ C/mol} \times (4 \times 10^{-7}) \text{ mol/cm}^3} \right)^2 = 80.5 \text{ s}^{-1}$$

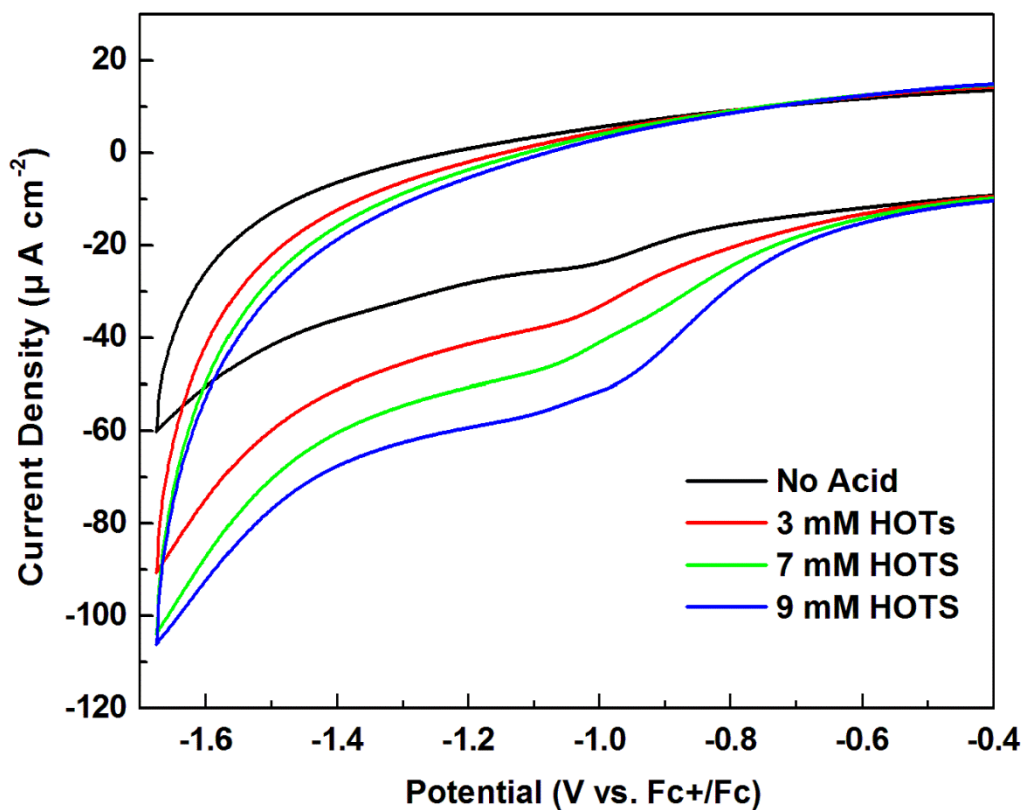


Figure S6. CV of **1** in the presence of HOTS. The catalytic onset for this compound was at a higher overpotential than that compared to **2**. H_2 was observed at $\eta > 350$ mV.

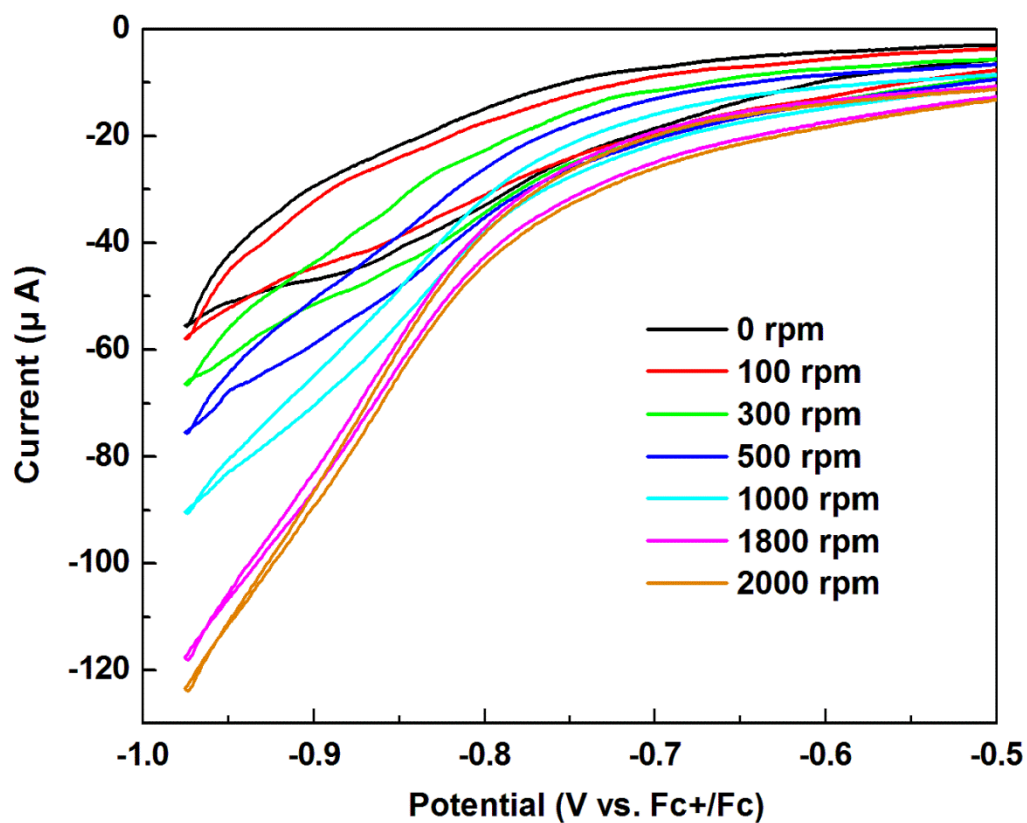


Figure S7. Proton reduction catalysis by compound **2** at various rotation rates of the rotating disk electrode (RDE). The RDE data was collected in order to construct the Koutecky-Levich plot displayed in Figure S8.

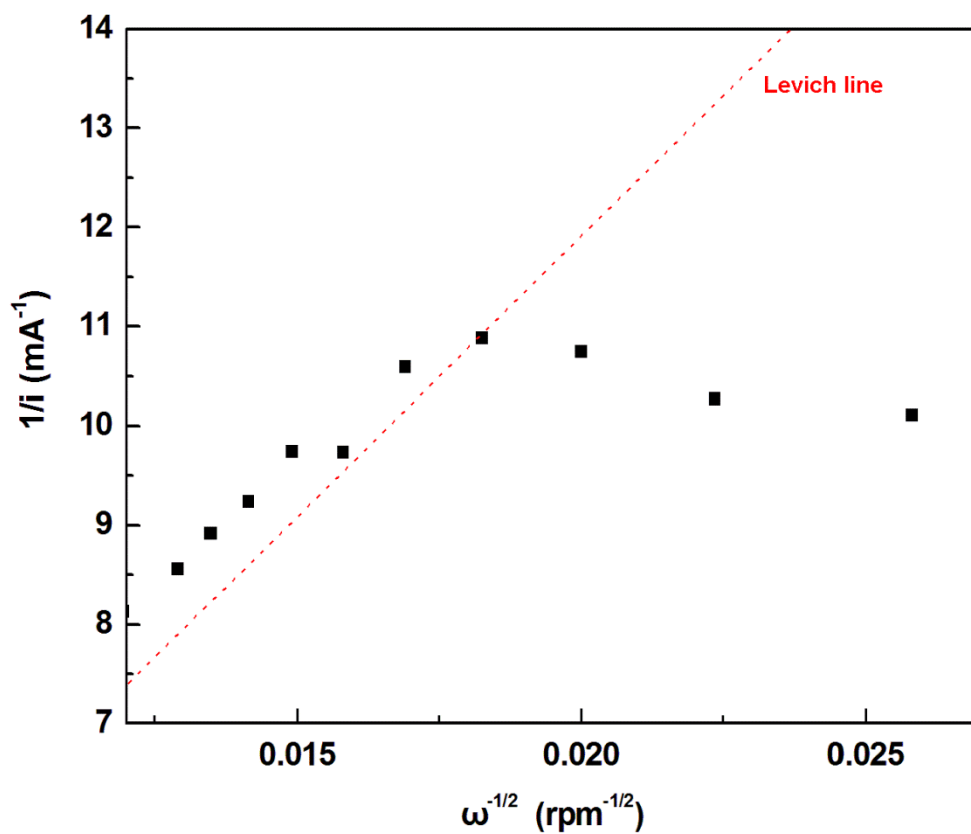


Figure S8. The Koutecky-Levich plot for the proton reduction catalysis of **2**. The deviation from the linear Levich line suggests that the concentration profile of the species responsible for the current changes as the diffusion layer thickness is varied due to the rotation rate. Such behavior is less likely to be observed for electrode-bound active species. For a detailed discussion, see reference 2.

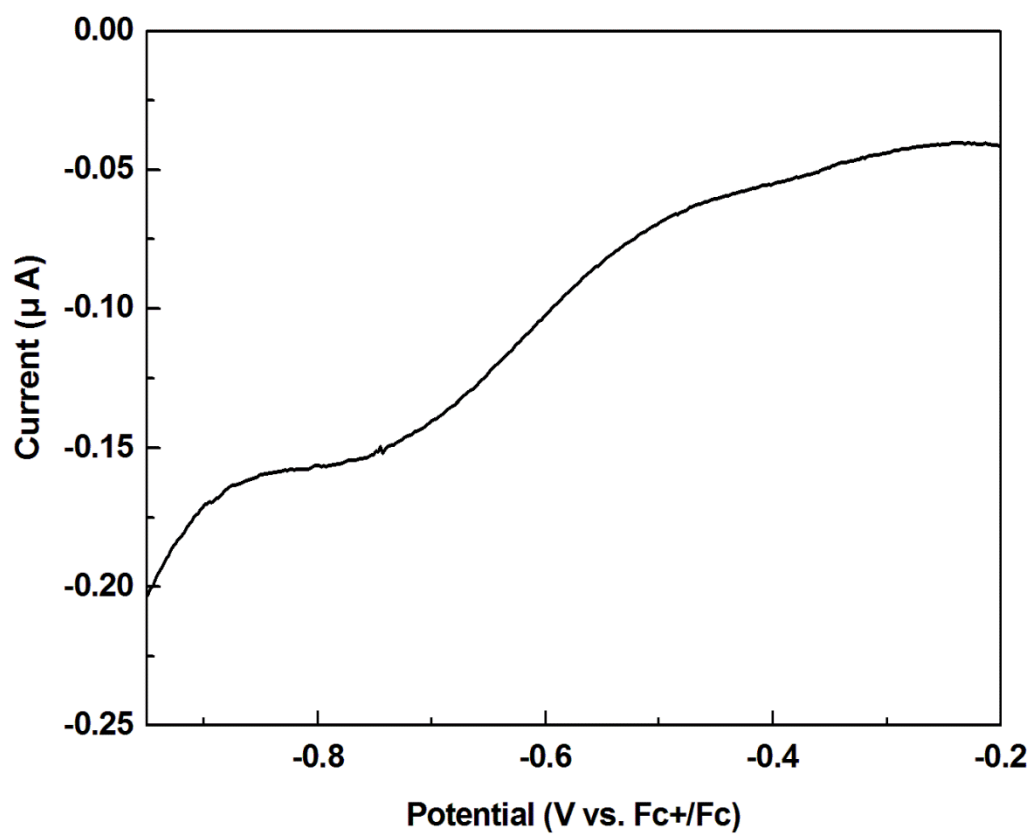


Figure S9. DPV trace of **2** with stoichiometric amount of acid. The reduction event for the protonated form of **2** can be seen at ca -710 mV, on top of which the catalytic current grows upon addition of acid.

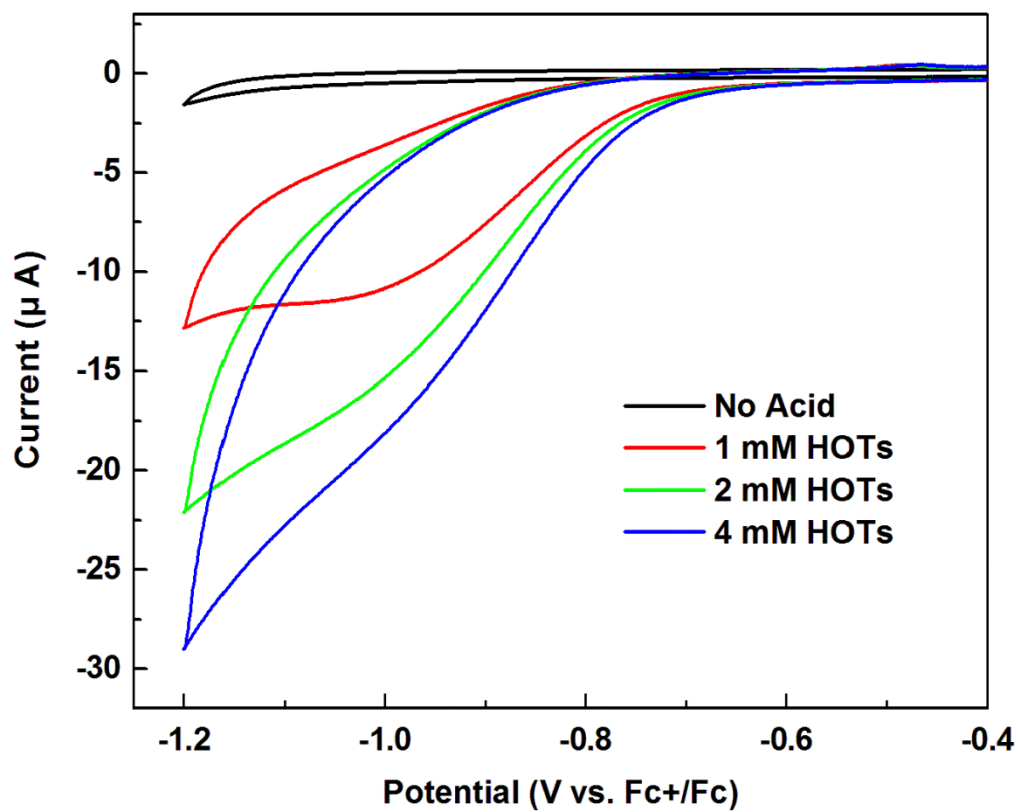


Figure S10. CV of $[\text{Co}(\text{tpm})_2] \cdot 2\text{BF}_4$ in the presence of HOTs. Proton reduction is observed at high overpotentials, similar to that for **1**.

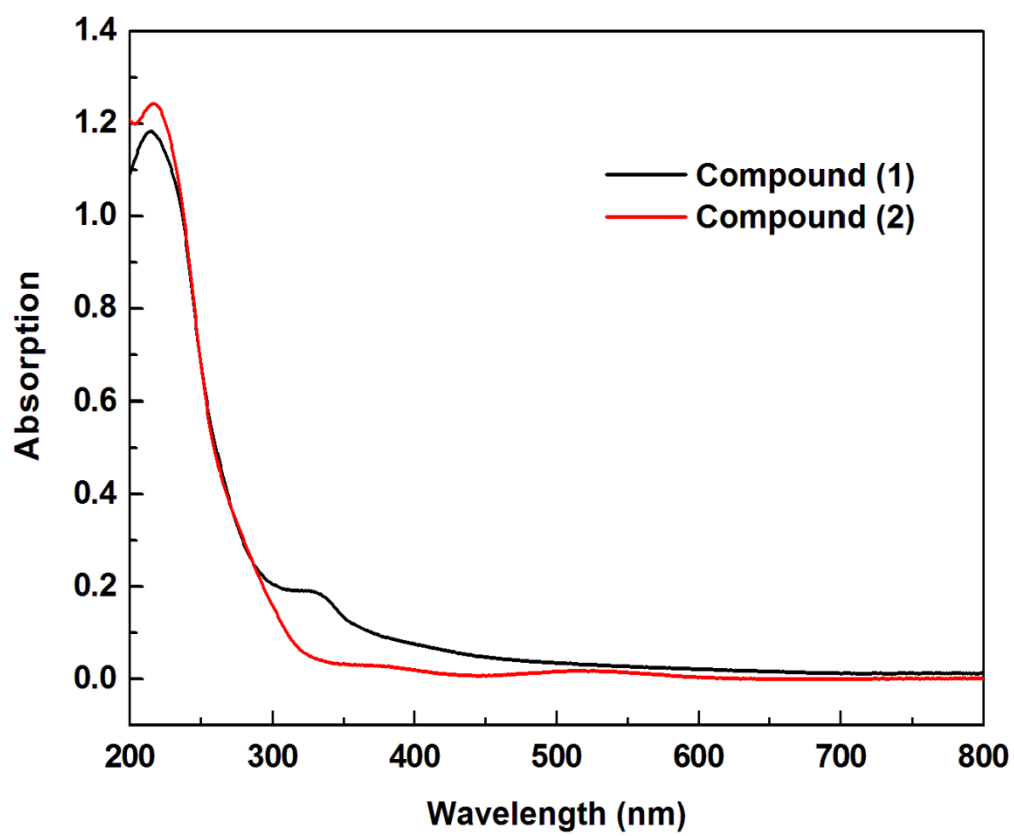


Figure S11. UV-vis spectra of compounds 1 and 2.

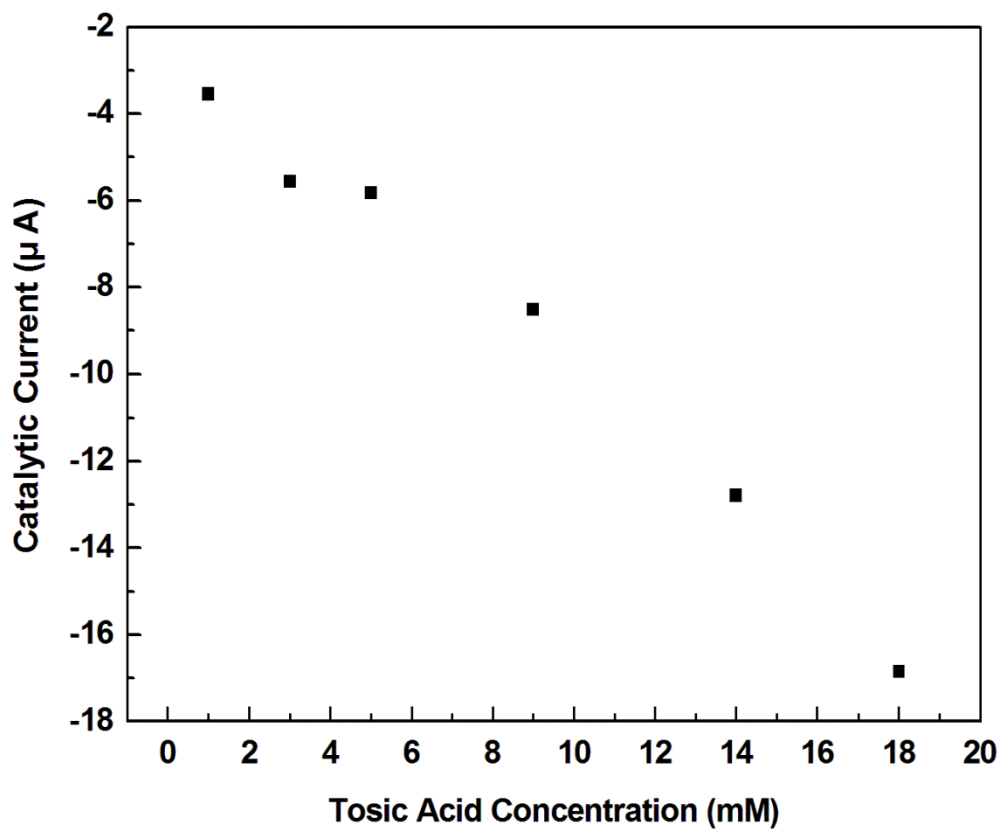


Figure S12. The catalytic current as a function of tonic acid concentration. A linear growth in current was observed.

Table S1. Crystal data and structure refinement for **1**.

Identification code	shelxl	
Empirical formula	C ₅₄ H ₁₀₂ B ₂ Co ₃ F ₈ O ₁₈	
Formula weight	1389.77	
Temperature	138(2) K	
Wavelength	0.71073 Å	
Crystal system	Triclinic	
Space group	P -1	
Unit cell dimensions	a = 9.938(2) Å	a = 102.448(4)°.
	b = 12.360(3) Å	b = 98.325(4)°.
	c = 15.263(4) Å	g = 105.752(4)°.
Volume	1720.3(7) Å ³	
Z	1	
Density (calculated)	1.34 Mg/m ³	
Absorption coefficient	0.798 mm ⁻¹	
F(000)	733	
Crystal size	0.10 x 0.10 x 0.03 mm ³	
Theta range for data collection	1.40 to 25.42°.	
Index ranges	-11<=h<=11, -14<=k<=14, -18<=l<=18	
Reflections collected	39368	
Independent reflections	6275 [R(int) = 0.0930]	
Completeness to theta = 25.42°	99.0 %	
Absorption correction	Semi-empirical from equivalents	
Max. and min. transmission	0.9700 and 0.9047	
Refinement method	Full-matrix least-squares on F ²	
Data / restraints / parameters	6275 / 0 / 394	
Goodness-of-fit on F ²	1.021	
Final R indices [I>2sigma(I)]	R1 = 0.0656, wR2 = 0.1548	
R indices (all data)	R1 = 0.1107, wR2 = 0.1825	
Largest diff. peak and hole	0.837 and -0.709 e.Å ⁻³	

Table S2. Atomic coordinates ($\times 10^4$) and equivalent isotropic displacement parameters ($\text{\AA}^2 \times 10^3$) for **1**. $U(\text{eq})$ is defined as one third of the trace of the orthogonalized U^{ij} tensor.

	x	y	z	U(eq)
C(1)	7382(6)	4515(4)	4789(4)	45(1)
C(2)	7043(5)	3476(4)	5172(3)	34(1)
C(3)	7305(5)	2363(4)	4732(3)	34(1)
C(4)	8917(5)	2602(5)	4826(4)	44(1)
C(5)	6537(6)	1931(4)	3724(3)	43(1)
C(6)	2986(6)	2566(5)	7642(4)	53(2)
C(7)	3874(5)	2311(4)	6961(4)	37(1)
C(8)	3219(5)	1745(4)	5953(3)	35(1)
C(9)	2739(6)	2639(5)	5539(4)	46(1)
C(10)	1972(5)	665(5)	5851(4)	44(1)
C(11)	9466(6)	2004(5)	8182(4)	49(2)
C(12)	8190(5)	1760(5)	7451(3)	35(1)
C(13)	7046(5)	575(4)	7132(3)	34(1)
C(14)	6483(6)	286(5)	7966(3)	43(1)
C(15)	7715(6)	-324(5)	6697(4)	46(1)
C(16)	1795(12)	527(10)	9486(6)	124(4)
C(17)	3064(12)	149(12)	9498(7)	150(5)
C(18)	2754(11)	-778(9)	8748(9)	141(5)
C(19)	1305(10)	-989(8)	8212(7)	105(3)
C(20)	7713(13)	5318(9)	10008(8)	137(4)
C(21)	6725(16)	4655(10)	10448(7)	139(5)
C(22)	6430(13)	3428(8)	9935(5)	126(4)
C(24)	7213(9)	6623(6)	7086(5)	81(2)
C(25)	7356(8)	7260(6)	8075(5)	70(2)
C(26)	5834(8)	6906(6)	8189(5)	72(2)
C(27)	5245(8)	5690(6)	7600(5)	69(2)
C(105)	7931(9)	4477(8)	9231(7)	120(4)
O(1)	6525(4)	3505(3)	5891(3)	54(1)
O(2)	6780(3)	1509(3)	5196(2)	30(1)
O(3)	5250(4)	2568(3)	7205(3)	56(1)

O(4)	4282(3)	1443(3)	5508(2)	30(1)
O(5)	7962(4)	2533(3)	7066(3)	53(1)
O(6)	5902(3)	612(3)	6480(2)	29(1)
O(9)	6009(5)	5591(4)	6891(3)	70(1)
O(10)	6833(6)	3447(4)	9092(3)	85(2)
O(11)	833(7)	-112(5)	8644(4)	109(2)
Co(1)	5000	0	5000	28(1)
Co(2)	6154(1)	2095(1)	6257(1)	30(1)
F(1)	9927(5)	4439(5)	13358(3)	108(2)
F(2)	7963(5)	3748(4)	12297(3)	102(2)
F(3)	9980(8)	4455(9)	11935(5)	218(5)
F(4)	9052(7)	5606(4)	12680(5)	160(3)
B(1)	9222(8)	4548(7)	12560(5)	55(2)

Table S3. Bond lengths [\AA] and angles [$^\circ$] for **1**.

C(1)-C(2)	1.500(7)
C(2)-O(1)	1.276(6)
C(2)-C(3)	1.502(7)
C(3)-O(2)	1.421(5)
C(3)-C(5)	1.523(7)
C(3)-C(4)	1.527(7)
C(6)-C(7)	1.495(7)
C(7)-O(3)	1.294(6)
C(7)-C(8)	1.510(7)
C(8)-O(4)	1.424(6)
C(8)-C(10)	1.516(7)
C(8)-C(9)	1.532(7)
C(11)-C(12)	1.476(7)
C(12)-O(5)	1.277(6)
C(12)-C(13)	1.518(7)
C(13)-O(6)	1.416(6)
C(13)-C(15)	1.526(7)
C(13)-C(14)	1.536(7)
C(16)-O(11)	1.410(10)
C(16)-C(17)	1.457(13)
C(17)-C(18)	1.363(12)
C(18)-C(19)	1.475(12)
C(19)-O(11)	1.374(9)
C(20)-C(21)	1.441(14)
C(20)-C(105)	1.484(12)
C(21)-C(22)	1.477(13)
C(22)-O(10)	1.405(9)
C(24)-O(9)	1.432(7)
C(24)-C(25)	1.511(9)
C(25)-C(26)	1.503(10)
C(26)-C(27)	1.481(9)
C(27)-O(9)	1.412(7)
C(105)-O(10)	1.385(9)

O(1)-Co(2)	1.902(4)
O(2)-Co(2)	1.888(3)
O(2)-Co(1)	2.124(3)
O(3)-Co(2)	1.882(4)
O(4)-Co(2)	1.895(3)
O(4)-Co(1)	2.132(3)
O(5)-Co(2)	1.894(4)
O(6)-Co(2)	1.892(3)
O(6)-Co(1)	2.188(3)
Co(1)-O(2)#1	2.124(3)
Co(1)-O(4)#1	2.132(3)
Co(1)-O(6)#1	2.188(3)
Co(1)-Co(2)#1	2.7036(8)
Co(1)-Co(2)	2.7036(8)
F(1)-B(1)	1.367(8)
F(2)-B(1)	1.310(8)
F(3)-B(1)	1.303(9)
F(4)-B(1)	1.341(9)
O(1)-C(2)-C(1)	121.1(5)
O(1)-C(2)-C(3)	117.2(4)
C(1)-C(2)-C(3)	121.7(4)
O(2)-C(3)-C(2)	109.1(4)
O(2)-C(3)-C(5)	109.7(4)
C(2)-C(3)-C(5)	109.8(4)
O(2)-C(3)-C(4)	109.1(4)
C(2)-C(3)-C(4)	108.5(4)
C(5)-C(3)-C(4)	110.7(4)
O(3)-C(7)-C(6)	121.6(5)
O(3)-C(7)-C(8)	116.4(4)
C(6)-C(7)-C(8)	122.0(5)
O(4)-C(8)-C(7)	108.9(4)
O(4)-C(8)-C(10)	110.4(4)
C(7)-C(8)-C(10)	109.2(4)
O(4)-C(8)-C(9)	108.5(4)

C(7)-C(8)-C(9)	108.1(4)
C(10)-C(8)-C(9)	111.6(4)
O(5)-C(12)-C(11)	122.4(5)
O(5)-C(12)-C(13)	116.0(4)
C(11)-C(12)-C(13)	121.6(5)
O(6)-C(13)-C(12)	109.5(4)
O(6)-C(13)-C(15)	110.1(4)
C(12)-C(13)-C(15)	108.4(4)
O(6)-C(13)-C(14)	109.1(4)
C(12)-C(13)-C(14)	108.5(4)
C(15)-C(13)-C(14)	111.2(4)
O(11)-C(16)-C(17)	107.0(8)
C(18)-C(17)-C(16)	106.9(9)
C(17)-C(18)-C(19)	109.4(9)
O(11)-C(19)-C(18)	105.9(7)
C(21)-C(20)-C(105)	107.3(9)
C(20)-C(21)-C(22)	104.5(9)
O(10)-C(22)-C(21)	106.7(8)
O(9)-C(24)-C(25)	105.7(5)
C(26)-C(25)-C(24)	102.2(6)
C(27)-C(26)-C(25)	102.7(6)
O(9)-C(27)-C(26)	107.7(6)
O(10)-C(105)-C(20)	105.6(8)
C(2)-O(1)-Co(2)	114.5(4)
C(3)-O(2)-Co(2)	113.6(3)
C(3)-O(2)-Co(1)	139.2(3)
Co(2)-O(2)-Co(1)	84.53(12)
C(7)-O(3)-Co(2)	114.9(4)
C(8)-O(4)-Co(2)	113.2(3)
C(8)-O(4)-Co(1)	142.1(3)
Co(2)-O(4)-Co(1)	84.11(12)
C(12)-O(5)-Co(2)	115.5(3)
C(13)-O(6)-Co(2)	113.7(3)
C(13)-O(6)-Co(1)	139.9(3)
Co(2)-O(6)-Co(1)	82.65(11)

C(27)-O(9)-C(24)	109.2(5)
C(105)-O(10)-C(22)	107.7(6)
C(19)-O(11)-C(16)	109.8(7)
O(2)#1-Co(1)-O(2)	180.00(13)
O(2)#1-Co(1)-O(4)#1	74.56(12)
O(2)-Co(1)-O(4)#1	105.44(12)
O(2)#1-Co(1)-O(4)	105.44(12)
O(2)-Co(1)-O(4)	74.56(12)
O(4)#1-Co(1)-O(4)	180.00(17)
O(2)#1-Co(1)-O(6)#1	73.98(11)
O(2)-Co(1)-O(6)#1	106.02(11)
O(4)#1-Co(1)-O(6)#1	73.67(12)
O(4)-Co(1)-O(6)#1	106.33(12)
O(2)#1-Co(1)-O(6)	106.02(11)
O(2)-Co(1)-O(6)	73.98(11)
O(4)#1-Co(1)-O(6)	106.33(12)
O(4)-Co(1)-O(6)	73.67(12)
O(6)#1-Co(1)-O(6)	180.000(1)
O(2)#1-Co(1)-Co(2)#1	44.03(8)
O(2)-Co(1)-Co(2)#1	135.97(8)
O(4)#1-Co(1)-Co(2)#1	44.21(8)
O(4)-Co(1)-Co(2)#1	135.79(8)
O(6)#1-Co(1)-Co(2)#1	43.96(8)
O(6)-Co(1)-Co(2)#1	136.04(8)
O(2)#1-Co(1)-Co(2)	135.97(8)
O(2)-Co(1)-Co(2)	44.03(8)
O(4)#1-Co(1)-Co(2)	135.79(8)
O(4)-Co(1)-Co(2)	44.21(8)
O(6)#1-Co(1)-Co(2)	136.04(8)
O(6)-Co(1)-Co(2)	43.96(8)
Co(2)#1-Co(1)-Co(2)	180.0
O(3)-Co(2)-O(2)	171.35(16)
O(3)-Co(2)-O(6)	92.21(16)
O(2)-Co(2)-O(6)	86.71(13)
O(3)-Co(2)-O(5)	93.28(18)

O(2)-Co(2)-O(5)	95.17(16)
O(6)-Co(2)-O(5)	85.00(16)
O(3)-Co(2)-O(4)	85.45(16)
O(2)-Co(2)-O(4)	85.92(14)
O(6)-Co(2)-O(4)	86.30(13)
O(5)-Co(2)-O(4)	171.16(16)
O(3)-Co(2)-O(1)	96.03(18)
O(2)-Co(2)-O(1)	85.09(16)
O(6)-Co(2)-O(1)	171.76(16)
O(5)-Co(2)-O(1)	94.88(17)
O(4)-Co(2)-O(1)	93.96(15)
O(3)-Co(2)-Co(1)	121.65(12)
O(2)-Co(2)-Co(1)	51.44(9)
O(6)-Co(2)-Co(1)	53.38(9)
O(5)-Co(2)-Co(1)	122.94(13)
O(4)-Co(2)-Co(1)	51.67(10)
O(1)-Co(2)-Co(1)	120.95(12)
F(3)-B(1)-F(2)	111.5(8)
F(3)-B(1)-F(4)	106.4(7)
F(2)-B(1)-F(4)	109.3(6)
F(3)-B(1)-F(1)	109.8(7)
F(2)-B(1)-F(1)	108.9(6)
F(4)-B(1)-F(1)	110.9(7)

Symmetry transformations used to generate equivalent atoms:

#1 -x+1,-y,-z+1

Table S4. Anisotropic displacement parameters ($\text{\AA}^2 \times 10^3$) for **1**. The anisotropic displacement factor exponent takes the form: $-2p^2 [h^2 a^* U^{11} + \dots + 2 h k a^* b^* U^{12}]$

	U ¹¹	U ²²	U ³³	U ²³	U ¹³	U ¹²
C(1)	58(4)	27(3)	48(3)	12(2)	12(3)	5(3)
C(2)	32(3)	30(3)	36(3)	10(2)	7(2)	3(2)
C(3)	31(3)	27(3)	41(3)	14(2)	8(2)	2(2)
C(4)	38(3)	34(3)	56(3)	11(3)	17(3)	6(2)
C(5)	51(3)	35(3)	38(3)	11(2)	12(3)	4(3)
C(6)	52(4)	49(4)	57(4)	5(3)	23(3)	13(3)
C(7)	35(3)	24(3)	54(3)	8(2)	17(2)	10(2)
C(8)	34(3)	34(3)	40(3)	9(2)	13(2)	15(2)
C(9)	47(3)	42(3)	59(4)	16(3)	12(3)	25(3)
C(10)	32(3)	38(3)	57(3)	8(3)	11(3)	7(2)
C(11)	37(3)	48(3)	54(3)	13(3)	0(3)	7(3)
C(12)	32(3)	38(3)	39(3)	15(2)	8(2)	13(2)
C(13)	30(3)	32(3)	39(3)	11(2)	2(2)	8(2)
C(14)	42(3)	42(3)	39(3)	14(2)	4(2)	3(3)
C(15)	46(3)	37(3)	51(3)	7(3)	1(3)	19(3)
C(16)	136(9)	156(10)	78(6)	-11(6)	2(6)	87(8)
C(17)	125(9)	236(15)	84(7)	-11(8)	-11(6)	109(10)
C(18)	85(7)	115(9)	184(12)	-40(8)	3(7)	45(6)
C(19)	102(7)	82(6)	118(7)	-7(5)	8(6)	42(6)
C(20)	143(10)	72(7)	131(9)	-38(6)	7(8)	-6(6)
C(21)	216(15)	135(10)	77(7)	11(7)	17(8)	95(10)
C(22)	218(12)	95(7)	51(5)	15(5)	42(6)	26(7)
C(24)	102(6)	41(4)	97(6)	11(4)	46(5)	14(4)
C(25)	84(5)	39(4)	76(5)	10(3)	16(4)	8(4)
C(26)	98(6)	49(4)	73(5)	10(3)	34(4)	24(4)
C(27)	67(4)	62(4)	74(5)	4(4)	20(4)	23(4)
C(105)	63(5)	86(6)	151(9)	-35(6)	12(5)	-14(5)
O(1)	50(2)	45(2)	61(3)	14(2)	7(2)	10(2)
O(2)	30(2)	24(2)	38(2)	11(1)	12(1)	8(1)
O(3)	55(3)	42(2)	68(3)	16(2)	16(2)	11(2)

O(4)	25(2)	25(2)	41(2)	8(1)	8(1)	7(1)
O(5)	51(2)	52(3)	54(2)	10(2)	15(2)	13(2)
O(6)	29(2)	23(2)	35(2)	10(1)	5(1)	6(1)
O(9)	82(3)	43(3)	81(3)	2(2)	31(3)	19(2)
O(10)	103(4)	76(3)	44(3)	-4(2)	5(3)	-4(3)
O(11)	114(5)	101(4)	100(4)	-13(4)	-19(4)	68(4)
Co(1)	26(1)	22(1)	35(1)	7(1)	7(1)	5(1)
Co(2)	29(1)	22(1)	36(1)	6(1)	7(1)	5(1)
F(1)	102(4)	126(4)	99(3)	43(3)	2(3)	44(3)
F(2)	79(3)	61(3)	139(4)	32(3)	5(3)	-15(2)
F(3)	185(7)	430(14)	209(7)	229(9)	159(6)	193(8)
F(4)	156(5)	51(3)	222(7)	38(4)	-73(5)	7(3)
B(1)	43(4)	49(4)	69(5)	25(4)	4(4)	8(3)

Table S5. Hydrogen coordinates ($\times 10^4$) and isotropic displacement parameters ($\text{\AA}^2 \times 10^3$) for **1**.

	x	y	z	U(eq)
H(1A)	6598	4416	4279	68
H(1B)	8271	4586	4567	68
H(1C)	7500	5221	5271	68
H(4A)	9394	2898	5478	65
H(4B)	9283	3185	4501	65
H(4C)	9107	1878	4560	65
H(5A)	6592	1151	3462	64
H(5B)	6994	2468	3387	64
H(5C)	5530	1896	3672	64
H(6A)	2353	1832	7693	80
H(6B)	2409	3030	7437	80
H(6C)	3615	3004	8243	80
H(9A)	3574	3311	5596	69
H(9B)	2057	2898	5868	69
H(9C)	2279	2280	4888	69
H(10A)	1598	255	5198	66
H(10B)	1215	893	6113	66
H(10C)	2297	147	6175	66
H(11A)	10179	2733	8190	73
H(11B)	9874	1363	8062	73
H(11C)	9191	2079	8778	73
H(14A)	6139	913	8265	65
H(14B)	7256	211	8403	65
H(14C)	5693	-451	7764	65
H(15A)	6971	-1081	6432	68
H(15B)	8443	-397	7168	68
H(15C)	8162	-72	6212	68
H(16A)	1355	372	10007	149
H(16B)	2053	1373	9538	149

H(17A)	3894	790	9469	180
H(17B)	3299	-83	10069	180
H(18A)	2802	-1481	8947	169
H(18B)	3464	-615	8362	169
H(19A)	1337	-964	7571	126
H(19B)	663	-1761	8203	126
H(20A)	8635	5754	10450	164
H(20B)	7316	5884	9781	164
H(21A)	5834	4873	10406	166
H(21B)	7158	4787	11104	166
H(22A)	6989	3045	10283	151
H(22B)	5399	2993	9831	151
H(24A)	7047	7113	6673	97
H(24B)	8091	6418	7004	97
H(25A)	7979	7006	8500	84
H(25B)	7746	8115	8178	84
H(26A)	5792	6939	8838	87
H(26B)	5310	7409	7974	87
H(27A)	5357	5138	7967	83
H(27B)	4214	5507	7336	83
H(10D)	7884	4762	8673	143
H(10E)	8874	4359	9386	143

References

1. H. Burger, U. Wannagat, *Monatsh. Chem.* 1963, **94**, 1007.
2. A. J. Bard, L. R. Faulkner, *Electrochemical Methods: Fundamentals and Applications 2nd Ed.*, Wiley, New York, 2001.
3. A. J. Sathrum, C. P. Kubiak, *J. Phys. Chem. Lett.*, 2011, **2**, 2372.